

# We are IntechOpen, the world's leading publisher of Open Access books Built by scientists, for scientists

6,900

Open access books available

185,000

International authors and editors

200M

Downloads

Our authors are among the

154

Countries delivered to

TOP 1%

most cited scientists

12.2%

Contributors from top 500 universities



WEB OF SCIENCE™

Selection of our books indexed in the Book Citation Index  
in Web of Science™ Core Collection (BKCI)

Interested in publishing with us?  
Contact [book.department@intechopen.com](mailto:book.department@intechopen.com)

Numbers displayed above are based on latest data collected.  
For more information visit [www.intechopen.com](http://www.intechopen.com)



# Multi-sensorial Active Perception for Indoor Environment Modeling

Luz Abril Torres-Méndez

*Research Centre for Advanced Studies - Campus Saltillo  
Mexico*

## 1. Introduction

For many applications, the information provided by individual sensors is often incomplete, inconsistent, or imprecise. For problems involving detection, recognition and reconstruction tasks in complex environments, it is well known that no single source of information can provide the absolute solution, besides the computational complexity. The merging of multisource data can create a more consistent interpretation of the system of interest, in which the associated uncertainty is decreased.

Multi-sensor data fusion also known simply as sensor data fusion is a process of combining evidence from different information sources in order to make a better judgment (Llinas & Waltz, 1990; Hall, 1992; Klein, 1993). Although, the notion of data fusion has always been around, most multisensory data fusion applications have been developed very recently, converting it in an area of intense research in which new applications are being explored constantly. On the surface, the concept of fusion may look to be straightforward but the design and implementation of fusion systems is an extremely complex task. Modeling, processing, and integrating of different sensor data for knowledge interpretation and inference are challenging problems. These problems become even more difficult when the available data is incomplete, inconsistent or imprecise.

In robotics and computer vision, the rapid advance of science and technology combined with the reduction in the costs of sensor devices, has caused that these areas together, and before considered as independent, strength the diverse needs of each. A central topic of investigation in both areas is the recovery of the tridimensional structure of large-scale environments. In a large-scale environment the complete scene cannot be captured from a single referential frame or given position, thus an active way of capturing the information is needed. In particular, having a mobile robot able to build a 3D map of the environment is very appealing since it can be applied to many important applications. For example, virtual exploration of remote places, either for security or efficiency reasons. These applications depend not only on the correct transmission of visual and geometric information but also on the quality of the information captured. The latter is closely related to the notion of active perception as well as the uncertainty associated to each sensor. In particular, the behavior any artificial or biological system should follow to accomplish certain tasks (e.g., extraction,

simplification and filtering), is strongly influenced by the data supplied by its sensors. This data is in turn dependent on the perception criteria associated with each sensorial input (Conde & Thalmann, 2004).

A vast body of research on 3D modeling and virtual reality applications has been focused on the fusion of intensity and range data with promising results (Pulli et al., 1997; Stamos & Allen, 2000) and recently (Guidi et al., 2009). Most of these works consider the complete acquisition of 3D points from the object or scene to be modeled, focusing mainly on the registration and integration problems.

In the area of computer vision, the idea of extracting the shape or structure from an image has been studied since the end of the 70's. Scientists in computer vision were mainly interested in methods that reflect the way the human eye works. These methods, known as "shape-from-X", extract depth information by using visual patterns of the images, such as shading, texture, binocular vision, motion, among others. Because of the type of sensors used in these methods, they are categorized as passive sensing techniques, i.e., data is obtained without emitting energy and involve typically mathematical models of the image formation and how to invert them. Traditionally, these models are based on physical principles of the light interaction. However, due to the difficulties to invert them, is necessary to assume several aspects about the physical properties of the objects in the scene, such as the type of surface (Lambertian, matte) and *albedo*, which cannot be suitable to real complex scenes.

In the robotics community, it is common to combine information from different sensors, even using the same sensors repeatedly over time, with the goal of building a model of the environment. Depth inference is frequently achieved by using sophisticated, but costly, hardware solutions. Range sensors, in particular laser rangefinders, are commonly used in several applications due to its simplicity and reliability (but not its elegance, cost and physical robustness). Besides of capturing 3D points in a direct and precise manner, range measurements are independent of external lighting conditions. These techniques are known as active sensing techniques. Although these techniques are particularly needed in non-structured environments (e.g., natural outdoors, aquatic environments), they are not suitable for capturing complete 2.5D maps with a resolution similar to that of a camera. The reason for this is that these sensors are extremely expensive or, in other way, impractical, since the data acquisition process may be slow and normally the spatial resolution of the data is limited. On the other hand, intensity images have a high resolution which allows precise results in well-defined objectives. These images are easy to acquire and give texture maps in real color images.

However, although many elegant algorithms based on traditional approaches for depth recovery have been developed, the fundamental problem of obtaining precise data is still a difficult task. In particular, achieving geometric correctness and realism may require data collection from different sensors as well as the correct fusion of all these observations.

Good examples are the stereo cameras that can produce volumetric scans that are economical. However, these cameras require calibration or produce range maps that are incomplete or of limited resolution. In general, using only 2D intensity images will provide

sparse measurements of the geometry which are non-reliable unless some simple geometry about the scene to model is assumed. By fusing 2D intensity images with range finding sensors, as first demonstrated in (Jarvis, 1992), a solution to 3D vision is realized - circumventing the problem of inferring 3D from 2D.

One aspect of great importance in the 3D modeling reconstruction is to have a fast, efficient and simple data acquisition process from the sensors and yet, have a good and robust reconstruction. This is crucial when dealing with dynamic environments (e.g., people walking around, illumination variation, etc.) and systems with limited battery-life. We can simplify the way the data is acquired by capturing only partial but reliable range information of regions of interest. In previous research work, the problem of tridimensional scene recovery using incomplete sensorial data was tackled for the first time, specifically, by using intensity images and a limited number of range data (Torres-Méndez & Dudek, 2003; Torres-Méndez & Dudek, 2008). The main idea is based on the fact that the underlying geometry of a scene can be characterized by the visual information and its interaction with the environment together with its inter-relationships with the available range data. Figure 1 shows an example of how a complete and dense range map is estimated from an intensity image and the associated partial depth map. These statistical relationships between the visual and range data were analyzed in terms of small patches or neighborhoods of pixels, showing that the contextual information of these relationships can provide information to infer complete and dense range maps. The dense depth maps with their corresponding intensity images are then used to build 3D models of large-scale man-made indoor environments (offices, museums, houses, etc.)

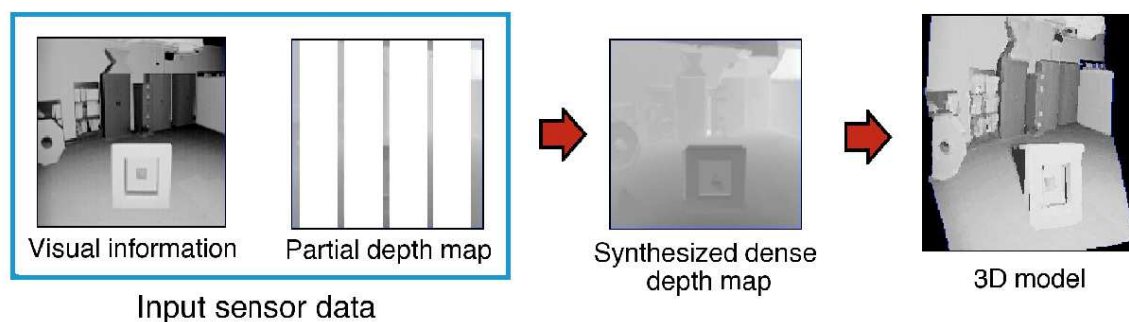


Fig. 1. An example of the range synthesis process. The data fusion of intensity and incomplete range is carried on to reconstruct a 3D model of the indoor scene. Image taken from (Torres-Méndez, 2008).

In that research work, the sampling strategies for measuring the range data was determined beforehand and remain fixed (vertical and horizontal lines through the scene) during the data acquisition process. These sampling strategies sometimes carried on critical limitations to get an ideal reconstruction as the quality of the input range data, in terms of the geometric characteristics it represent, did not capture the underlying geometry of the scene to be modeled. As a result, the synthesis process of the missing range data was very poor.

In the work presented in this chapter, we solve the above mentioned problem by selecting in an optimal way the regions where the initial (minimal) range data must be captured. Here, the term *optimal* refers in particular, to the fact that the range data to be measured must truly

represent relevant information about the geometric structure. Thus, the input range data, in this case, must be good enough to estimate, together with the visual information, the rest of the missing range data.

Both sensors (camera and laser) must be fused (i.e., registered and then integrated) in a common reference frame. The fusion of visual and range data involves a number of aspects to be considered as the data is not of the same nature with respect to their resolution, type and scale. The images of real scene, i.e., those that represent a meaningful concept in their content, depend on the regularities of the environment in which they are captured (Van Der Schaaf, 1998). These regularities can be, for example, the natural geometry of objects and their distribution in space; the natural distributions of light; and the regularities that depend on the viewer's position. This is particularly difficult considering the fact that at each given position the mobile robot must capture a number of images and then analyze the optimal regions where the range data should be measured. This means that the laser should be directed to those regions with accuracy and then the incomplete range data must be registered with the intensity images before applying the statistical learning method to estimate complete and dense depth maps.

The statistical studies of these images can help to understand these regularities, which are not easily acquired from physical or mathematical models. Recently, there has been some success when using statistical methods to computer vision problems (Freeman & Torralba, 2002; Srivastava et al., 2003; Torralba & Oliva, 2002). However, more studies are needed in the analysis of the statistical relationships between intensity and range data. Having meaningful statistical tendencies could be of great utility in the design of new algorithms to infer the geometric structure of objects in a scene.

The outline of the chapter is as follows. In Section 2 we present related work to the problem of 3D environment modeling focusing on approaches that fuse intensity and range images. Section 3 presents our multi-sensorial active perception framework which statistically analyzes natural and indoor images to capture the initial range data. This range data together with the available intensity will be used to efficiently estimate dense range maps. Experimental results under different scenarios are shown in Section 4 together with an evaluation of the performance of the method.

## 2. Related Work

For the fundamental problem in computer vision of recovering the geometric structure of objects from 2D images, different monocular visual cues have been used, such as shading, defocus, texture, edges, etc. With respect to binocular visual cues, the most common are the obtained from stereo cameras, from which we can compute a depth map in a fast and economical way. For example, the method proposed in (Wan & Zhou, 2009), uses stereo vision as a basis to estimate dense depth maps of large-scale scenes. They generate depth map mosaics, with different angles and resolutions which are combined later in a single large depth map. The method presented in (Malik and Choi, 2008) is based in the shape from focus approach and use a defocus measure based in an optic transfer function implemented in the Fourier domain. In (Miled & Pesquet, 2009), the authors present a novel method based on stereo that help to estimate depth maps of scene that are subject to changes

in illumination. Other works propose to combine different methods to obtain the range maps. For example, in (Scharstein & Szeliski, 2003) a stereo vision algorithm and structured light are used to reconstruct scenes in 3D. However, the main disadvantage of above techniques is that the obtained range maps are usually incomplete or of limited resolution and in most of the cases a calibration is required.

Another way of obtaining a dense depth map is by using range sensors (e.g., laser scanners), which obtain geometric information in a direct and reliable way. A large number of possible 3D scanners are available on the market. However, cost is still the major concern and the more economical tend to be slow. An overview of different systems available to 3D shape of objects is presented in (Blais, 2004), highlighting some of the advantages and disadvantages of the different methods. Laser Range Finders directly map the acquired data into a 3D volumetric model thus having the ability to partly avoid the correspondence problem associated with visual passive techniques. Indeed, scenes with no textural details can be easily modeled. Moreover, laser range measurements do not depend on scene illumination.

More recently, techniques based on learning statistics have been used to recover the geometric structure from 2D images. For humans, to interpret the geometric information of a scene by looking to one image is not a difficult task. However, for a computational algorithm this is difficult as some *a priori* knowledge about the scene is needed.

For example, in (Torres-Méndez & Dudek, 2003) it was presented for the first time a method to estimate dense range map based on the statistical correlation between intensity and available range as well as edge information. Other studies developed more recently as in (Saxena & Chung, 2008), show that it is possible to recover the missing range data in the sparse depth maps using statistical learning approaches together with the appropriate characteristics of objects in the scene (e.g., edges or cues indicating changes in depth). Other works combine different types of visual cues to facilitate the recovery of depth information or the geometry of objects of interest.

In general, no matter what approach is used, the quality of the results will strongly depend on the type of visual cues used and the preprocessing algorithms applied to the input data.

### 3. The Multi-sensorial Active Perception Framework

This research work focuses on recovering the geometric (depth) information of a man-made indoor scene (e.g., an office, a room) by fusing photometric and partial geometric information in order to build a 3D model of the environment.

Our data fusion framework is based on an active perception technique that captures the limited range data in regions statistically detected from the intensity images of the same scene. In order to do that, a perfect registration between the intensity and range data is required. The registration process we use is briefly described in Section 3.2. After registering the partial range with the intensity data we apply a statistical learning method to estimate the unknown range and obtain a dense range map. As the mobile robot moves at different locations to capture information from the scene, the final step is to integrate all the dense range maps (together with intensity) and build a 3D map of the environment.

The key role of our active perception process concentrates on capturing range data from places where the visual cues of the images show depth discontinuities. Man-made indoor environments have inherent geometric and photometric characteristics that can be exploited to help in the detection of this type of visual cues.

First, we apply a statistical analysis on an image database to detect regions of interest on which range data should be acquired. With the internal representation, we can assign confidence values according to the ternary values obtained. These values will indicate the filling order of the missing range values. And finally, we use a non-parametric range synthesis method in (Torres-Méndez & Dudek, 2003) to estimate the missing range values and obtain a dense depth map. In the following sections, all these stages are explained in more detail.

### 3.1 Detecting regions of interest from intensity images

We wish to capture limited range data in order to simplify the data acquisition process. However, in order to have a good estimation of the unknown range, the quality of this initial range data is crucial. That is, it should represent the depth discontinuities existing in the scene. Since we have only information from images, we can apply a statistical analysis on the images and extract changes in depth.

Given that our method is based on a statistical analysis, the type of images to analyze in the database must contain characteristics and properties similar to the scenes of interest, as we focus on man-made scenes, we should have images containing those types of images. However, we start our experiments using a public available image database, the van Hateren database, which contains scenes of natural images. As this database contains important changes in depth in their scenes, this turns out to be the main characteristic to be considered so that our method can be functional.

The statistical analysis of small patches implemented is based in part on the Feldman and Yunes algorithm (Feldman & Yunes, 2006). This algorithm extracts characteristics of interest from an image through the observation of an image database and obtains an internal representation that concentrates the relevant information in a form of a ternary variable. To generate the internal representation we follow three steps. First, we reduce (in scale) the images in the database (see Figure 2). Then, each image is divided in patches of same size (e.g. 13 x13 pixels), with these patches we make a new database which is decomposed in its principal components by applying PCA to extract the most representative information, which is usually contained, in the first five eigenvectors. In Figure 3, the eigenvectors are depicted. These eigenvectors are the filters that are used to highlight certain characteristics on the intensity images, specifically the regions with relevant geometric information.

The last step consists on applying a threshold in order to map the images onto a ternary variable where we assign  $-1$  value to very low values,  $1$  to high values and  $0$  otherwise. This way, we can obtain an internal representation

$$\xi_i : G \rightarrow \{-1,0,1\}^k, \quad (1)$$

where  $k$  represents the number of filters (eigenvectors).  $G$  is the set of pixels of the scaled image.



Fig. 2. Some of the images taken from the van Hateren database. These images are reduced by a scaled factor of 2.

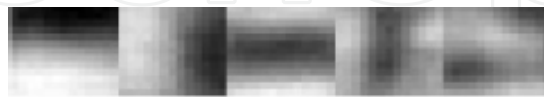


Fig. 3. The first 5 eigenvectors (zoomed out). These eigenvectors are used as filters to highlight relevant geometric information.

The internal representation gives information about the changes in depth as it is shown in Figure 4. It can be observed that, depending on the filter used, the representation gives a different orientation on the depth discontinuities in the scene. For example, if we use the first filter, the highlighted changes are the horizontal ones. If we applied the second filter, the discontinuities obtained are the vertical ones.



Fig. 4. The internal representation after the input image is filtered.

This internal representation is the basis to capture the initial range data from which we can obtain a dense range map.

### 3.2 Obtaining the registered sparse depth map

In order to obtain the initial range data we need to register the camera and laser sensors, i.e., the corresponding reference frame of the intensity image taken from the camera with the reference frame of the laser rangefinder. Our data acquisition system consists of a high resolution digital camera and a 2D laser rangefinder (laser scanner), both mounted on a pan unit and on top of a mobile robot. Registering different types of sensor data, which have different projections, resolutions and scaling properties is a difficult task. The simplest and easiest way to facilitate this sensor-to-sensor registration is to vertically align their center of projections (optical center for the camera and mirror center for the laser) are aligned to the center of projection of the pan unit. Thus, both sensors can be registered with respect to a common reference frame. The laser scanner and camera sensors work with different coordinate systems and they must be adjusted one to another. The laser scanner delivers spherical coordinates whereas the camera puts out data in a typical image projection. Once the initial the range data is collected we apply a post-registration algorithm which uses their projection types in order to do an image mapping.

The image-based registration algorithm is similar to that presented in (Torres-Méndez & Dudek, 2008) and assumes that the optical center of the camera and the mirror center of the laser scanner are vertically aligned and the orientation of both rotation axes coincide (see Figure 5). Thus, we only need to transform the panoramic camera data into the laser coordinate system. Details of the algorithm we use are given in (Torres-Méndez & Dudek, 2008).

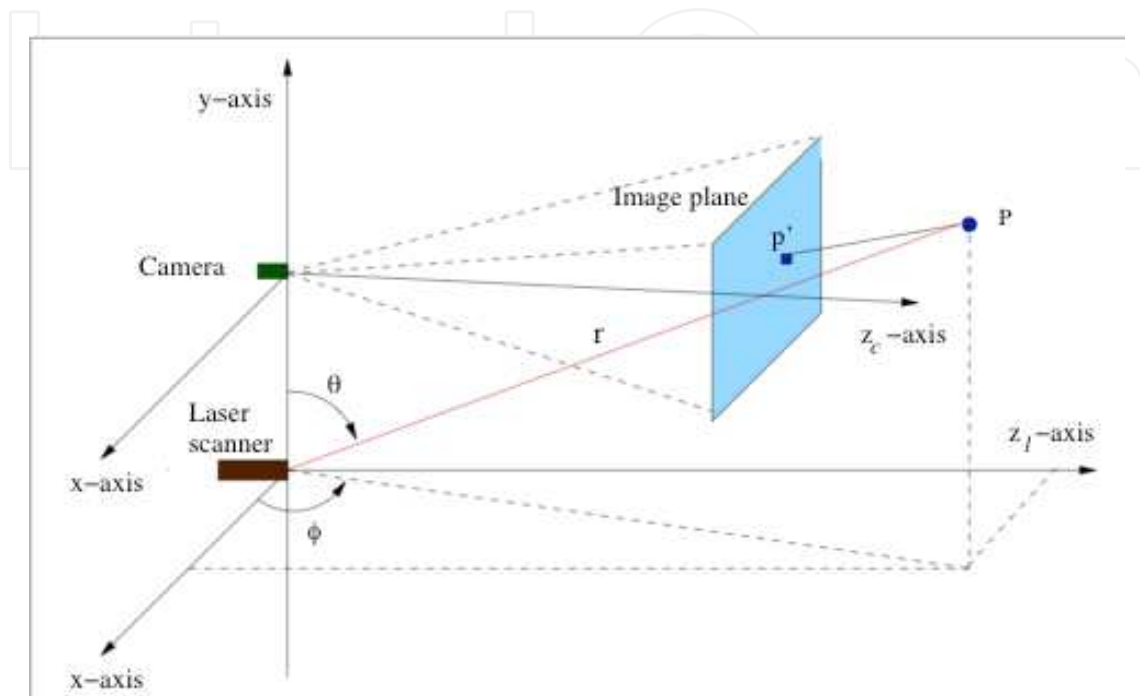


Fig. 5. Camera and laser scanner orientation and world coordinate system. Image taken from (Torres-Méndez & Dudek, 2008).

### 3.3 The range synthesis method

After obtaining the internal representation and a registered sparse depth map, we can apply the range synthesis method in (Torres-Méndez & Dudek, 2008). In general, the method estimates dense depth maps using intensity and partial range information. The Markov Random Field (MRF) model is trained using the (local) relationships between the observed range data and the variations in the intensity images and then used to compute the unknown range values. The Markovianity condition describes the local characteristics of the pixel values (in intensity and range, called voxels). The range value at a voxel depends only on neighboring voxels which have direct interactions on each other. We describe the non-parametric method in general and skip the details of the basis of MRF; the reader is referred to (Torres-Méndez & Dudek, 2008) for further details.

In order to compute the maximum *a posteriori* (MAP) for a depth value  $R_i$  of a voxel  $V_i$ , we need first to build an approximate distribution of the conditional probability  $P(f_i | f_{N_i})$  and sample from it. For each new depth value  $R_i \in R$  to estimate, the samples that correspond to

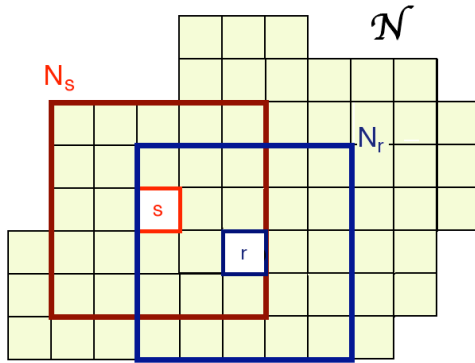


Fig. 6. A sketch of the neighborhood system definition.

the neighborhood system of voxel  $i$ , i.e.,  $N_i$ , are taken and the distribution of  $R_i$  is built as a histogram of all possible values that occur in the sample. The neighborhood system  $N_i$  (see Figure 6) is an infinite real subset of voxels, denoted by  $\mathcal{N}_{real}$ . Taking the MRF model as a basis, it is assumed that the depth value  $R_i$  depends only on the intensity and range values of its immediate neighbors defined in  $N_i$ . If we define a set

$$\Gamma(R_i) = \{N^* \subset \mathcal{N}_{real} : \|N_i - N^*\| = 0\}, \quad (2)$$

that contains all occurrences of  $N_i$  in  $\mathcal{N}_{real}$ , then the conditional probability distribution of  $R_i$  can be estimated through a histogram based on the depth values of voxels representing each  $N_i$  in  $\Gamma(R_i)$ . Unfortunately, the sample is finite and there exists the possibility that no neighbor has exactly the same characteristics in intensity and range, for that reason we use the heuristic of finding the most similar value in the available finite sample  $\Gamma'(R_i)$ , where  $\Gamma'(R_i) \subseteq \Gamma(R_i)$ . Now, let  $A_p$  be a local neighborhood system for voxel  $p$ , which is composed for neighbors that are located within radius  $r$  and is defined as:

$$A_p = \{A_q \in N \mid \text{dist}(p, q) \leq r\}. \quad (3)$$

In the non-parametric approximation, the depth value  $R_p$  of voxel  $V_p$  with neighborhood  $N_p$ , is synthesized by selecting the most similar neighborhood  $N_{best}$  to  $N_p$ .

$$N_{best} = \arg \min \|N_p - A_q\|, A_q \in A_p. \quad (4)$$

All neighborhoods  $A_q$  in  $A_p$  that are similar to  $N_{best}$  are included in  $\Gamma'(R_p)$  as follows:

$$\|N_p - A_q\| < (1 - \varepsilon) \|N_p - N_{best}\|. \quad (5)$$

The similarity measure between two neighborhoods  $N_a$  and  $N_b$  is described over the partial data of the two neighborhoods and is calculated as follows:

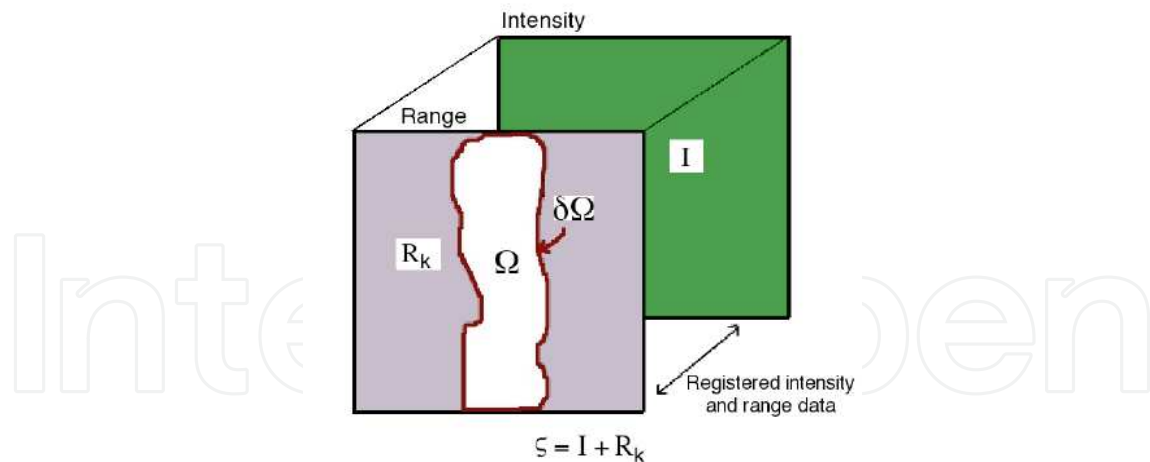


Fig. 7. The notation diagram. Taken from (Torres-Méndez, 2008).

$$\|N_a - N_b\| = \sum_{\vec{v} \in N_a, N_b} G(\sigma, \vec{v} - \vec{v}_0) \cdot D \quad (6)$$

$$D = \sqrt{(I_{\vec{v}}^a - I_{\vec{v}}^b)^2 + (R_{\vec{v}}^a - R_{\vec{v}}^b)^2}, \quad (7)$$

where  $\vec{v}_0$  represents the voxel located in the center of the neighborhood  $N_a$  and  $N_b$ ,  $\vec{v}$  is the neighboring pixel of  $\vec{v}_0$ .  $I_a$  and  $R_a$  are the intensity and range values to be compared.  $G$  is a Gaussian kernel that is applied to each neighborhood so that voxels located near the center have more weight than those located far from it. In this way we can build a histogram of depth values  $R_p$  in the center of each neighborhood in  $\Gamma'(R_i)$ .

### 3.3.1 Computing the priority values to establish the filling order

To achieve a good estimation for the unknown depth values, it is critical to establish an order to select the next voxel to synthesize. We base this order on the amount of available information at each voxel's neighborhood, so that the voxel with more neighboring voxels with already assigned intensity and range is synthesized first. We have observed that the reconstruction in areas with discontinuities is very problematic and a probabilistic inference is needed in these regions. Fortunately, such regions are identified by our internal representation (described in Section 3.1) and can be used to assign priority values. For example, we assign a high priority to voxels which ternary value is 1, so these voxels are synthesized first; and a lower priority to voxels with ternary value 0 and -1, so they are synthesized at the end.

The region to be synthesized is indicated by  $\Omega = \{w_i | i \in A\}$ , where  $w_i = R(x_i, y_i)$  is the unknown depth value located at pixel coordinates  $(x_i, y_i)$ . The input intensity and the known range value together conform the source region and is indicated by  $\zeta$  (see Figure 6). This region is used to calculate the statistics between the input intensity and range for the reconstruction. If  $V_p$  is the voxel with an unknown range value, inside  $\Omega$  and  $N_p$  is its neighborhood, which

is an  $n \times n$  window centered at  $V_p$ , then for each voxel  $V_p \in \Omega$ , we calculate its priority value as follows

$$P(V_p) = \frac{\sum_{i \in N_p} C(V_i)F(V_i)}{|N_p| - 1}, \quad (8)$$

where  $|N_p|$  indicates the total number of voxels in  $N_p$ . Initially, the priority value of  $C(V_i)$  for each voxel  $V_p \in \Omega$  is assigned a value of 1 if the associated ternary value is 1, 0.8 if its ternary value is 0 and 0.2 if -1.  $F(V_i)$  is a flag function, which takes value 1 if the intensity and range values of  $V_i$  are known, and 0 if its range value is unknown. In this way, voxels with greater priority are synthesized first.

### 3.4 Integration of dense range maps

We have mentioned that at each position the mobile robot takes an image, computes its internal representation to direct the laser range finder on the regions detected and capture range data. In order to produce a complete 3D model or representation of a large environment, we need to integrate *dense* panoramas with depth from multiple viewpoints. The approach taken is based on a hybrid method similar to that in (Torres-Méndez & Dudek, 2008) (the reader is advised to refer to the article for further details).

In general, the integration algorithm combines a geometric technique, which is a variant of the ICP algorithm (Besl & McKay, 1992) that matches 3D range scans, and an image-based technique, the SIFT algorithm (Lowe, 1999), that matches intensity features on the images. Since dense range maps with its corresponding intensity images are given as an input, their integration to a common reference frame is easier than having only intensity or range data separately.

## 4. Experimental Results

In order to evaluate the performance of the method, we use three databases, two of which are available on the web. One is the Middlebury database (Hiebert-Treuer, 2008) which contains intensity and dense range maps of 12 different indoor scenes containing objects with a great variety of texture. The other is the USF database from the CESAR lab at Oak Ridge National Laboratory. This database has intensity and dense range maps of indoor scenes containing regular geometric objects with uniform textures. The third database was created by capturing images using a stereo vision system in our laboratory. The scenes contain regular geometric objects with different textures. As we have ground truth range data from the public databases, we first simulate sparse range maps by eliminating some of the range information using different sampling strategies that follows different patterns (squares, vertical and horizontal lines, etc.) The sparse depth maps are then given as an input to our algorithm to estimate dense range maps. In this way, we can compare the ground-truth dense range maps with those synthesized by our method and obtain a quality measure for the reconstruction.

To evaluate our results we compute a well-know metric, called mean absolute residual (MAR) error. The MAR error of two matrices  $R_1$  and  $R_2$  is defined as

$$\text{MAR} = \frac{\sum_{i,j} |R_1(i,j) - R_2(i,j)|}{\# \text{ unknown range voxels}} \quad (9)$$

In general, just computing the MAR error is not a good mechanism to evaluate the success of the method. For example, when there are few results with a high MAR error, the average of the MAR error elevates. For this reason, we also compute the absolute difference at each pixel and show the result as an image, so we can visually evaluate our performance.

In all the experiments, the size of the neighborhood  $N$  is  $3 \times 3$  pixels for one experimental set and  $5 \times 5$  pixels for other. The search window varies between 5 and 10 pixels. The missing range data in the sparse depth maps varies between 30% and 50% of the total information.

#### 4.1 Range synthesis on sparse depth maps with different sampling strategies

In the following experiments, we have used the two first databases described above. For each of the input range maps in the databases, we first simulate a sparse depth map by eliminating a given amount of range data from these dense maps. The areas with missing depth values follow an arbitrary pattern (vertical, horizontal lines, squares). The size of these areas depends on the amount of information that is eliminated for the experiment (from 30% up to 50%). After obtaining a simulated sparse depth map, we apply the proposed algorithm. The result is a synthesized dense range map. We compare our results with the ground truth range map computing the MAR error and also an image of the absolute difference at each pixel.

Figure 8 shows the experimental setup of one of the scenes in the Middlebury database. In 8b the ground truth range map is depicted. Figure 9 shows the synthesized results for different sampling strategies for the baby scene.

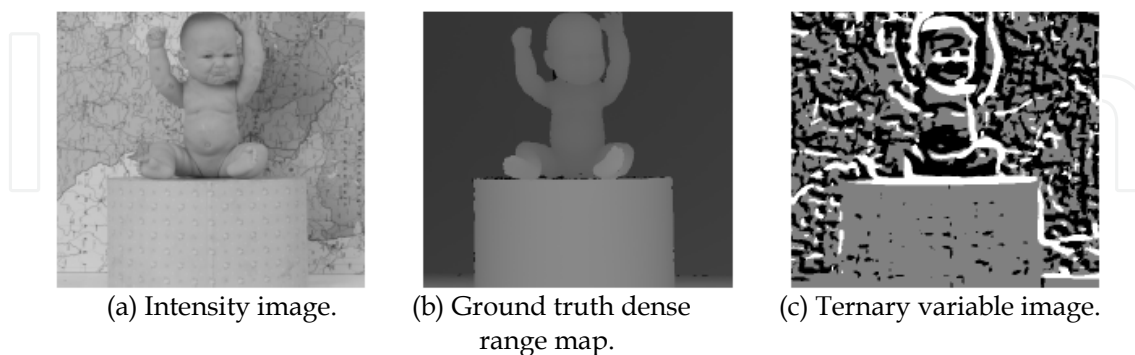


Fig. 8. An example of the experimental setup to evaluate the method (Middlebury database).



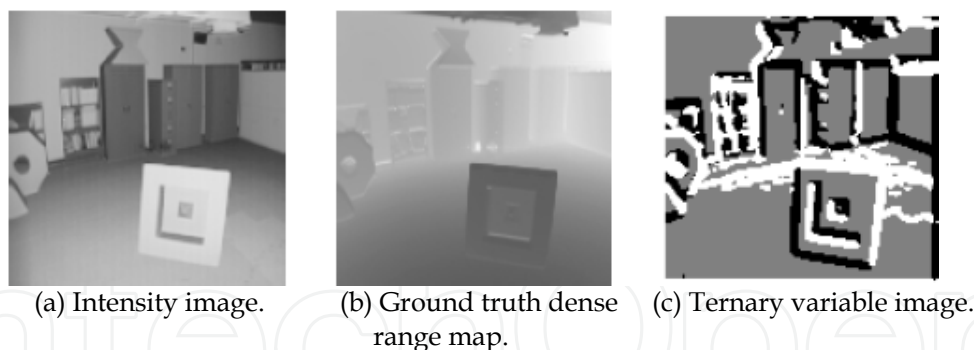


Fig. 10. An example of the experimental setup to evaluate the proposed method (USF database).

#### 4.2 Range synthesis on sparse depth maps obtained from the internal representation

We conducted experiments where the sparse depth maps contain range data only on regions indicated by the internal representation. Therefore, apart from greatly reducing the acquisition time, the initial range would represent all the relevant variations related to depth discontinuities in the scene. Thus, it is expected that the dense range map will be estimated more efficiently.

In Figure 10 an image from the USF database is shown with its corresponding ground truth range map and ternary variable image. In the USF database, contrary to the Middlebury database, the scenes are bigger and objects are located at different depths and the texture is uniform. Figure 10c depicts the ternary variable, which represents the initial range given as an input together with the intensity image to the range synthesis process. It can be seen that the discontinuities can be better appreciated in objects as they have a uniform texture. Figure 11 shows the synthesized dense range map. As before, the quality of the reconstruction depends on the available information. Good results are obtained as the known range is distributed around the missing range. It is important to determine which values inside the available information have greater influence on the reconstruction so we can give to them a high priority.

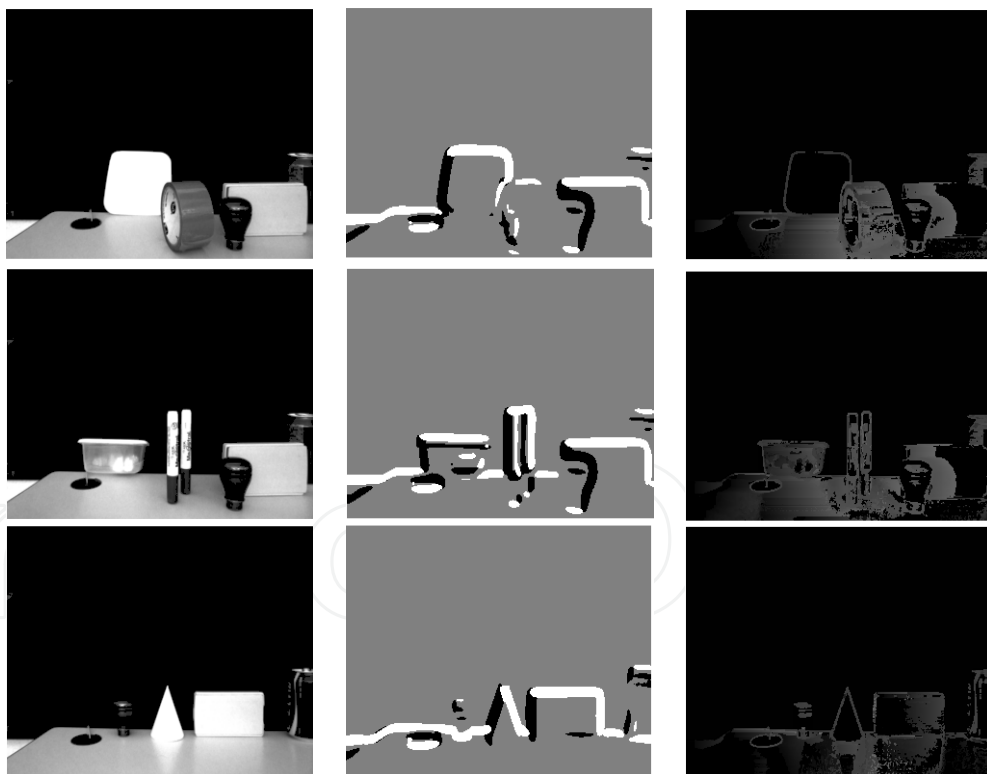
In general, the experimental results show that the ternary variable influences in the quality of the synthesis, especially in areas with depth discontinuities.



Fig. 11. The synthesized dense range map of the initial range values indicated in figure 10c.

### 4.3 Range synthesis on sparse depth maps obtained from stereo

We also test our method by using real sparse depth maps by acquiring pair of images directly from the stereo vision system, obtaining the sparse depth map, the internal representation and finally synthesizing the missing depth values in the map using the non-parametric MRF model. In Figure 12, we show the input data to our algorithm for three different scenes acquired in our laboratory. The left images of the stereo pair for each scene are shown in the first column. The sparse range maps depicted on Figure 12b are obtained from the Shirai's stereo algorithm (Klette & Schlus, 1998) using the epipolar geometry and the Harris corner detector (Harris & Stephens, 1988) as constraints. Figure 12c shows the ternary variable images used to compute the priority values to establish the synthesis order. In Figure 13, we show the synthesized results for each of the scenes shown in Figure 12. From top to bottom we show the synthesized results for iterations at different intervals. It can be seen that the algorithm first synthesizes the voxels with high priority, that is, the contours where depth discontinuities exists. This gives a better result as the synthesis process progresses. The results vary depending on the size of the neighborhood  $N$  and the size of the searching window  $d$ . On one hand, if  $N$  is more than  $5 \times 5$  pixels, it can be difficult to find a neighborhood with similar statistics. On the other hand, if  $d$  is big, for example, it considers the neighborhoods in the whole image, then the computing time increases accordingly.



(a) Left (stereo) image. (b) Ternary variable images. (c) Sparse depth maps.

Fig. 12. Input data for three scenes captured in our laboratory.

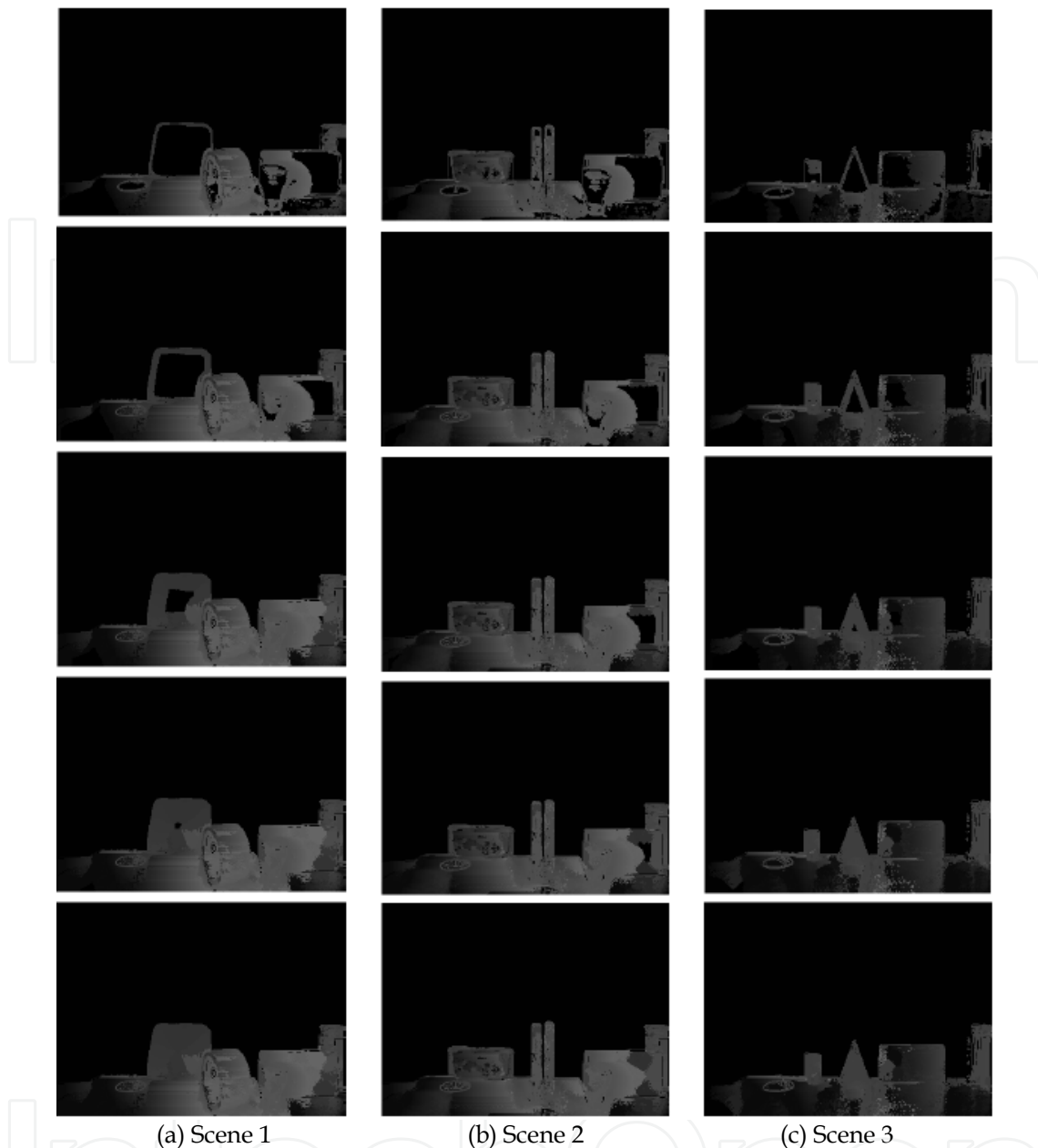


Fig. 13. Experimental results of the three different scenes shown in Figure 11. Each row shows the results at different steps of the range synthesis algorithm.

## 5. Conclusion

We have presented an approach to recover dense depth maps based on the statistical analysis of visual cues. The visual cues extracted represent regions indicating depth discontinuities in the intensity images. These are the regions where range data should be captured and represent the range data given as an input together with the intensity map to the range estimation process. Additionally, the internal representation of the intensity map is used to assign priority values to the initial range data. The range synthesis is improved as the orders in which the voxels are synthesized are established from these priority values.

The quality of the results depends on the amount and type of the initial range information, in terms of the variations captured on it. In other words, if the correlation between the intensity and range data available represents (although partially) the correlation of the intensity near regions with missing range data, we can establish the statistics to be looked for in such available input data.

Also, as in many non-deterministic methods, we have seen that the results depend on the suitable selection of some parameters. One is the neighborhood size ( $N$ ) and the other the radius of search ( $r$ ). With the method here proposed the synthesis near the edges (indicated by areas that present depth discontinuities) is improved compared to prior work in the literature.

While a broad variety of problems have been covered with respect to the automatic 3D reconstruction of unknown environments, there remain several open problems and unanswered questions. With respect to the data collection, a key issue in our method is the quality of the observable range data. In particular, with the type of the geometric characteristics that can be extracted in relation to the objects or scene that the range data represent. If the range data do not capture the inherent geometry of the scene to be modeled, then the range synthesis process on the missing range values will be poor. The experiments presented in this chapter were based on acquiring the initial range data in a more directed way such that the regions captured reflect important changes in the geometry.

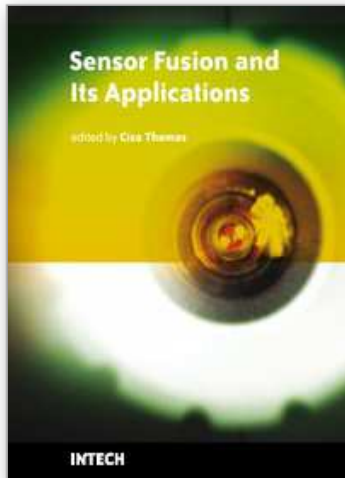
## 6. Acknowledgements

The author gratefully acknowledges financial support from CONACyT (CB-2006/55203).

## 7. References

- Besl, P.J. & McKay, N.D. (1992). A method for registration of 3D shapes. *IEEE Transactions on Pattern Analysis and Machine Intelligence*, Vol. 4, No. 2, 239-256, 1992.
- Blais, F. (2004). A review of 20 years of range sensor development. *Journal of Electronic Imaging*, Vol. 13, No. 1, 231-240, 2004.
- Conde, T. & Thalmann, D. (2004). An artificial life environment for autonomous virtual agents with multi-sensorial and multi-perceptive features. *Computer Animation and Virtual Worlds*, Vol. 15, 311-318, ISSN: 1546-4261.
- Feldman, T. & Younes, L. (2006). Homeostatic image perception: An artificial system. *Computer Vision and Image Understanding*, Vol. 102, No. 1, 70-80, ISSN:1077-3142.
- Freeman, W.T. & Torralba, A. (2002). Shape recipes: scene representations that refer to the image. *Adv. In Neural Information Processing Systems 15 (NIPS)*.
- Guidi, G. & Remondino, F. & Russo, M. & Menna, F. & Rizzi, A. & Ercoli, S. (2009). A Multi-Resolution Methodology for the 3D Modeling of Large and Complex Archeological Areas. *International Journal of Architectural Computing*, Vol. 7, No. 1, 39-55, Multi Science Publishing.
- Hall, D. (1992). *Mathematical Techniques in Multisensor Data Fusion*. Boston, MA: Artech House.
- Harris, C. & Stephens, M. (1988). A combined corner and edge detector. In *Fourth Alvey Vision Conference*, Vol. 4, pp. 147-151, 1988, Manchester, UK.
- Hiebert-Treuer, B. (2008). Stereo datasets with ground truth.

- <http://vision.middlebury.edu/stereo/data/scenes2006/>.
- Jarvis, R.A. (1992). 3D shape and surface colour sensor fusion for robot vision. *Robotica*, Vol. 10, 389–396.
- Klein, L.A. (1993). *Sensor and Data Fusion Concepts and Applications*. SPIE Opt. Engineering Press, Tutorial Texts, Vol. 14.
- Klette, R. & Schlens, K. (1998). *Computer vision: three-dimensional data from images*. Springer-Singapore. ISBN: 9813083719, 1998.
- Llinas, J. & Waltz, E. (1990). *Multisensor Data Fusion*. Boston, MA: Artech House.
- Lowe, D.G. (1999). Object recognition from local scale-invariant features. In *Proceedings of the International Conference on Computer Vision ICCV*, 1150–1157.
- Malik, A.S. & Choi, T.-S. (2007). Application of passive techniques for three dimensional cameras. *IEEE Transactions on Consumer Electronics*, Vol. 53, No. 2, 258–264, 2007.
- Malik, A. S. & Choi, T.-S. (2008). A novel algorithm for estimation of depth map using image focus for 3D shape recovery in the presence of noise. *Pattern Recognition*, Vol. 41, No. 7, July 2008, 2200–2225.
- Miled, W. & Pesquet, J.-C. (2009). A convex optimization approach for depth estimation under illumination variation. *IEEE Transactions on image processing*, Vol. 18, No. 4, 2009, 813–830.
- Pulli, K. & Cohen, M. & Duchamp, M. & Hoppe, H. & McDonald, J. & Shapiro, L. & Stuetzle, W. (1997). Surface modeling and display from range and color data. *Lectures Notes in Computer Science* 1310: 385–397, ISBN: 978-3-540-63507-9, Springer Berlin.
- Saxena, A. & Chung, S. H. (2008). 3D depth reconstruction from a single still image. *International journal of computer vision*, Vol. 76, No. 1, 2008, 53–69.
- Scharstein, D. & Szeliski, R. (2003). High-accuracy stereo depth maps using structured light. *IEEE Computer Society Conference on Computer Vision and Pattern Recognition*, Vol. 1, pp. 195–202.
- Stamos, I. & Allen, P.K. (2000). 3D model construction using range and image data. In *Proceedings of the International Conference on Vision and Pattern Recognition*, 2000.
- Srivastava, A., Lee, A.B., Simoncelli, E.P. & Zhu, S.C. (2003). On advances in statistical modeling of natural images. *Journal of the Optical Society of America*, Vol. 53, No. 3, 375–385, 2003.
- Torralba, A. & Oliva, A. (2002). Depth estimation from image structure. *IEEE Trans. Pattern Analysis and Machine Intelligence*, Vol. 24, No. 9, 1226–1238, 2002.
- Torres-Méndez, L. A. & Dudek, G. (2003). Statistical inference and synthesis in the image domain for mobile robot environment modeling. In *Proc. of the IEEE/RSJ Conference on Intelligent Robots and Systems*, Vol. 3, pp. 2699–2706, October, Las Vegas, USA.
- Torres-Méndez, L. A. & Dudek, G. (2008). Inter-Image Statistics for 3D Environment Modeling. *International Journal of Computer Vision*, Vol. 79, No. 2, 137–158, 2008. ISSN: 0920-5691.
- Torres-Méndez, L. A. (2008). *Inter-Image Statistics for Mobile Robot Environment Modeling*. VDM Verlag Dr. Muller, 2008, ISBN: 3639068157.
- Van Der Schaaf, A. (1998). *Natural Image Statistics and Visual Processing*. PhD thesis, Rijksuniversiteit Groningen, 1998.
- Wan, D. & Zhou, J. (2009). Multiresolution and wide-scope depth estimation using a dual-PTZ-camera system. *IEEE Transactions on Image Processing*, Vol. 18, No. 3, 677–682.



## **Sensor Fusion and its Applications**

Edited by Ciza Thomas

ISBN 978-953-307-101-5

Hard cover, 488 pages

**Publisher** Sciyo

**Published online** 16, August, 2010

**Published in print edition** August, 2010

This book aims to explore the latest practices and research works in the area of sensor fusion. The book intends to provide a collection of novel ideas, theories, and solutions related to the research areas in the field of sensor fusion. This book is a unique, comprehensive, and up-to-date resource for sensor fusion systems designers. This book is appropriate for use as an upper division undergraduate or graduate level text book. It should also be of interest to researchers, who need to process and interpret the sensor data in most scientific and engineering fields. The initial chapters in this book provide a general overview of sensor fusion. The later chapters focus mostly on the applications of sensor fusion. Much of this work has been published in refereed journals and conference proceedings and these papers have been modified and edited for content and style. With contributions from the world's leading fusion researchers and academicians, this book has 22 chapters covering the fundamental theory and cutting-edge developments that are driving this field.

### **How to reference**

In order to correctly reference this scholarly work, feel free to copy and paste the following:

Luz Abril Torres-Méndez (2010). Multisensorial Active Perception for Indoor Environment Modeling, Sensor Fusion and its Applications, Ciza Thomas (Ed.), ISBN: 978-953-307-101-5, InTech, Available from: <http://www.intechopen.com/books/sensor-fusion-and-its-applications/multisensorial-active-perception-for-indoor-environment-modeling->

**INTECH**  
open science | open minds

### **InTech Europe**

University Campus STeP Ri  
Slavka Krautzeka 83/A  
51000 Rijeka, Croatia  
Phone: +385 (51) 770 447  
Fax: +385 (51) 686 166  
[www.intechopen.com](http://www.intechopen.com)

### **InTech China**

Unit 405, Office Block, Hotel Equatorial Shanghai  
No.65, Yan An Road (West), Shanghai, 200040, China  
中国上海市延安西路65号上海国际贵都大饭店办公楼405单元  
Phone: +86-21-62489820  
Fax: +86-21-62489821

© 2010 The Author(s). Licensee IntechOpen. This chapter is distributed under the terms of the [Creative Commons Attribution-NonCommercial-ShareAlike-3.0 License](#), which permits use, distribution and reproduction for non-commercial purposes, provided the original is properly cited and derivative works building on this content are distributed under the same license.

IntechOpen

IntechOpen